IEICE TRANS. COMMUN., VOL.E93–B, NO.12 DECEMBER 2010

PAPER Special Section on Wireless Distributed Networks

Combined Nyquist and Compressed Sampling Method for Radio Wave Data Compression of a Heterogeneous Network System

Doohwan LEE[†a)], **Takayuki YAMADA**[†], **Hiroyuki SHIBA**[†], **Yo YAMAGUCHI**[†], ***Members***, ***and*** **Kazuhiro UEHARA**[†], ***Senior Member***

SUMMARY To satisfy the requirement of a unified platform which can flexibly deal with various wireless radio systems, we proposed and implemented a heterogeneous network system composed of distributed flexible access points and a protocol-free signal processing unit. Distributed flexible access points are remote RF devices which perform the reception of multiple types of radio wave data and transfer the received data to the protocol-free signal processing unit through wired access network. The protocol-free signal processing unit performs multiple types of signal analysis by software. To realize a highly flexible and efficient radio wave data reception and transfer, we employ the recently developed compressed sensing technology. Moreover, we propose a combined Nyquist and compressed sampling method for the decoding signals to be sampled at the Nyquist rate and for the sensing signals to be sampled at the compressed rate. For this purpose, the decoding signals and the sensing signals are converted into the intermediate band frequency (IF) and mixed. In the IF band, the decoding signals are set at lower center frequencies than those of the sensing signals. The down converted signals are sampled at the rate of four times of the whole bandwidth of the decoding signals plus two times of the whole bandwidth of the sensing signals. The purpose of above setting is to simultaneously conduct Nyquist rate and compressed rate sampling in a single ADC. Then, all of odd (or even) samples are preserved and some of even (or odd) samples are randomly discarded. This method reduces the data transfer burden in dealing with the sensing signals while guaranteeing the realization of Nyquist-rate decoding performance. Simulation and experiment results validate the efficiency of the proposed method.

key words: *compressed sensing, compressive sampling, heterogeneous network system, l1-minimization, cognitive radio*

1. Introduction

Rapid developments and changes of wireless radio environments require a unified platform which can flexibly deal with various wireless radio systems regardless of the individual wireless standard. Previously, a new network architecture called the appliance defined ubiquitous network (ADUN) had been proposed in which wireless appliances are connected by network without specific network protocol standards [1], [2]. Radio wave data rather than decoded signals of individual appliances are transferred over the ADUN. In the similar vein, we proposed and implemented a heterogeneous network system which is composed of distributed flexible access points and a protocol-free signal processing unit [3]. Distributed flexible access points are remote RF devices which have the capability of receiving a wide variety of wireless signals from several hundred Mega Hertz to several Giga Hertz. The protocol-free signal processing unit has the capability of performing multiple types of signal analysis.

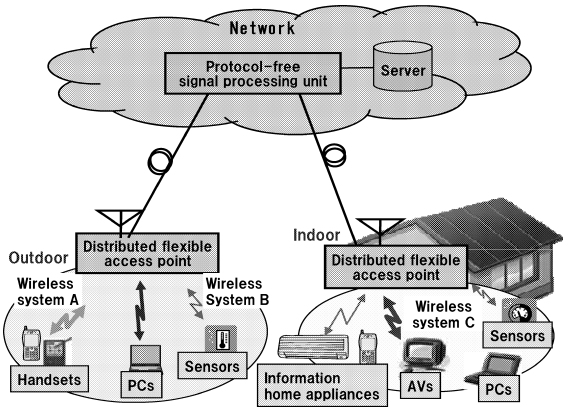

Fig. 1 A heterogeneous network system with distributed flexible access points and protocol-free signal processing unit.

Figure 1 illustrates the concept of the proposed heterogeneous network system. Multiple wirelesses signals are received at each distributed flexible access point. Received radio wave data are transferred to the protocol-free signal processing unit through wired access network such as an optical fiber network [4]. Similar approaches are found in the literature (ex. [5]–[7] and references therein), which transfer RF signals over radio-on-fiber network. The protocol-free signal processing unit performs multiple types of signal analysis by software exploiting software defined radio and cognitive radio technologies. If a new radio protocol is introduced, the protocol-free signal processing unit can also deal with the new radio protocol by software update. If necessary, previously stored data at servers can be also used for the highly elaborated signal analysis exploiting the past history of data.

To realize a highly flexible radio wave data reception at distributed flexible access points and an efficient radio wave data transfer between distributed flexible access points and the protocol-free signal processing unit, we employ the recently developed compressed sensing.

Compressed sensing is a new framework for solving an ill-posed inverse problem of the sparse signal [8]–[10]. It is used in various fields [11]–[13] including astronomy, magnetic resonance imaging, and digital imaging. All exploit the naturally sparsity of their underlying data. Compressed

Manuscript received April 21, 2010.
Manuscript revised August 2, 2010.

[†]The authors are with NTT Network Innovation Laboratories, NTT Corporation, Yokosuka-shi, 239-0847 Japan.
a) E-mail: lee.doohwan@lab.ntt.co.jp

DOI: 10.1587/transcom.E93.B.3238

sensing has been also researched in the wireless communication literature [14]–[20]. [14] utilized the sparse characteristics of the multipath channel profile to apply compressed sensing theory to ultra-wideband channel estimation. [15] used compressed sensing theory for occupied channel detection in wideband cognitive radio by utilizing the sparse nature of the frequency usage. It also applied the wavelet-based edge detection to make the spectrum sparser. By only detecting discontinuities of occupied channels, it further reduced the sampling cost. [16] derived the error bound of the compressed sensing based signal detection. [17] proposed the usage of Gabor time-frequency decomposition to sense the real GSM band signal by utilizing compressed sensing. [18] considered a cognitive wideband spectrum sensing in a distributed manner by exploiting the spatial diversity and joint sparsity. [19] and its extended version [20] proposed the parallel spectrum sensing for cognitive radios using parallel compressed sensing blocks.

Regarding the proposed heterogeneous network system, compressed sensing has following two advantages. First, compressed sensing provides universality in the wireless signal reception regardless of system types. This provides flexibility of the signal reception because multiple types of signals can be received by a unified signal reception method. Moreover, no hardware modifications are necessary even when new wireless systems are introduced. Second, compressed sensing enables signal reception and reconstruction at a lower rate than Nyquist rate. This reduces a burden of signal reception at distributed flexible access points, and also reduces a burden of data transfer between distributed flexible access points and the protocol-free signal processing unit.

Uniquely different from previous research on compressed sensing, we propose the combined Nyquist and compressed rate sampling method as follows: First, to decode the known signals (hereafter noted as decoding signals), Nyquist rate sampling is conducted to guarantee the performance. Second, to detect the unknown signals (hereafter noted as sensing signals), compressed rate sampling is conducted to reduce the sampling burden. Most importantly, both sampling methods are performed simultaneously by a single ADC. If the proposed method is not applied, at least two or more distinct sampling blocks are necessary for the Nyquist rate and compressed rate sampling. On the other hand, if the proposed method is applied, only a single sampling block is enough to provide the flexibility whether a certain signal is sampled by the Nyquist rate or compressed rate.

The detailed description of the proposed method is as follows: First, the decoding signals and the sensing signals are converted into the intermediate band frequency (IF) and mixed. In the IF band, the decoding signals are set at lower center frequencies than those of the sensing signals. Second, the down converted signals are sampled at the rate of four times of the whole bandwidth of the decoding signals plus two times of the whole bandwidth of the sensing signals. The purpose of above setting is to simultaneously conduct Nyquist rate and compressed rate sampling in a single ADC. Third, all of odd (or even) samples are preserved and some of even (or odd) samples are randomly discarded. Note that compressed sensing is only applied to the sensing signals while the conventional Nyquist sampling is conducted for the decoding signals. Therefore, the Nyquist-rate decoding performance is guaranteed for the decoding signals while the data transfer sampling burden of the sensing signals are reduced by compressed sensing.

For the full understanding of our approach, we provide the basic knowledge of compressed sensing. Then, the proposed sampling method is described. The remainder of this paper is organized as follow: Sect. 2 provides the basic theory of compressed sensing. Section 3 describes the system model and the proposed sampling method. Section 4 evaluates the performance of the proposed method by computer simulations and experiments. Finally, Sect. 5 concludes this paper.

2. Compressed Sensing

2.1 Basic Concept

Compressed sensing is a new theory that uses signal sparsity to reduce the amount of data that needs to be sampled [8]–[10]. The projection of an N-dimensional signal vector onto a K-dimensional ($K \ll N$) signal vector typically loses some information and the inverse problem (K equations with N variables) has an infinite number of solutions. However, when the signal has S-sparse representation ($S < K \ll N$) in some convenient basis and the projection matrix is incoherent with the basis, the inverse problem has, with high probability, a unique and exact solution.

2.2 Projection and Reconstruction

Let $N \times 1$ signal vector $\mathbf{X}$ be sparsely represented with an $N \times N$ basis matrix $\mathbf{\Psi}$ and $N \times 1$ sparse vector $\mathbf{s}$ as $\mathbf{X} = \mathbf{\Psi s}$. It follows that $K \times 1$ projection vector $\mathbf{Y}$ is obtained from $K \times N$ projection matrix $\mathbf{\Phi}$ as $\mathbf{Y} = \mathbf{\Phi X} = \mathbf{\Phi\Psi s}$. By defining the compressed sensing matrix $\mathbf{\Theta}$ as $\mathbf{\Phi\Psi}$, the equivalent notation $\mathbf{Y} = \mathbf{\Theta s}$ is given.

Typically, inverse problem $\mathbf{s} = \mathbf{\Theta}^{-1}\mathbf{Y}$ is ill-posed and not solvable. However, it has been proven that this inverse problem is cast to the following l1-norm minimization problem if $\mathbf{s}$ is sparse [21]–[23].

$$\min \|\tilde{\mathbf{s}}\|_1 \ \text{ subject to } \mathbf{Y} = \mathbf{\Theta}\tilde{\mathbf{s}} \ \text{ and } \ \tilde{\mathbf{s}} \in \mathbf{R}^n, \tag{1}$$

where, $\|\tilde{\mathbf{s}}\|_1 = \sum_i |\tilde{s}_i|$ and $\mathbf{R}^n$ is the set of $N \times 1$ vector.

This l1-norm minimization problem is solvable by the basis pursuit [24] or the iterative greedy algorithm [25]. If basis matrix $\mathbf{\Psi}$ and projection matrix $\mathbf{\Phi}$ satisfy the restricted isometry property, described below, the solution, $\tilde{\mathbf{s}}$, is unique and identical to $\mathbf{s}$ with overwhelming probability.

The number of projections depends not only on the size of the representation basis (N) but also on the amount of the information (S). In conventional transform coding, all

N transforms are performed regardless of the size of S, so the S most significant coefficients are searched. However, K $(= O(S \log N))$ projections are sufficient in compressed sensing, which is highly efficient given large N and small S and enables signal reception and reconstruction at a lower rate than Nyquist rate.

2.3 Restricted Isometry Property

The restricted isometry property (RIP) provides the sufficient condition of projection matrix $\mathbf{\Phi}$ and basis matrix $\mathbf{\Psi}$ for solving the l1-norm minimization problem [26], [27].

When compressed sensing matrix $\mathbf{\Theta}$ $(= \mathbf{\Phi\Psi})$ satisfies the following inequality for all S-sparse vectors, matrix $\mathbf{\Phi}$ is said to obey the RIP of order S.

$$(1 - \delta_s) \|\mathbf{s}\|_2^2 \leq \|\mathbf{\Theta s}\|_2^2 \leq (1 + \delta_s) \|\mathbf{s}\|_2^2, \tag{2}$$

where, $\|\mathbf{s}\|_2 = \sum_i s_i^2$ and δ_s $(0 \leq \delta_s < 1)$ is the smallest constant that satisfies Eq. (2).

In the geometrical sense, the Euclidian distance between any two S-sparse vectors in $\mathbf{R}^n$ is approximately preserved after projection when $\mathbf{\Phi}$ obeys the RIP of order S with δ_s.

2.4 Decoupled Projection from Reconstruction

For robust signal reconstruction, the projection matrix should be chosen to obey the RIP with the basis matrix. To provide universal nonadaptive projection, random matrices are typically used. It has been proven that the projection matrix that consists of random Gaussian ensemble, random Bernoulli ensemble, or randomly chosen rows of the Fourier transform matrix obeys the RIP with all types of basis matrices [28].

These universal projection matrices allow not only signal-independent projection, but also signal-independent reconstruction. Consider the following situation. After projection vector $\mathbf{Y}$ is obtained using $\mathbf{\Phi}$, it is realized that signal vector $\mathbf{X}$ can be more sparsely represented in the basis matrix $\mathbf{\Psi}'$. How can one deal with this situation? Surprisingly, one does not need to conduct the projection again since the l1-norm minimization problem can be solved with the previously obtained $\mathbf{Y}$ and a new $\mathbf{\Theta}'$ $(= \mathbf{\Phi\Psi}')$. This indicates that once the projection is performed, the reconstruction can be performed with any convenient basis matrix. In terms of the proposed heterogeneous network system, this can be also translated as follow: no hardware modifications at distributed flexible access points are necessary even when a new wireless system is introduced. This comes from the fact that the new wireless system can be reconstructed by the software calculation with new basis at the protocol-free signal processing unit.

3. Combined Nyquist and Compressed Sampling Method

This section proposes a new sampling method that combines the advantages of the Nyquist rate sampling and compressed rate sampling.

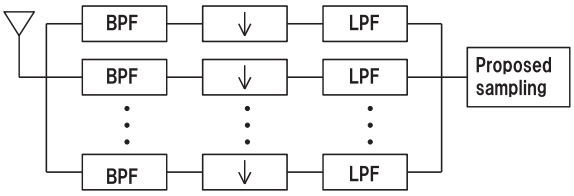

Fig. 2 Simplified block diagram of a distributed flexible access point.

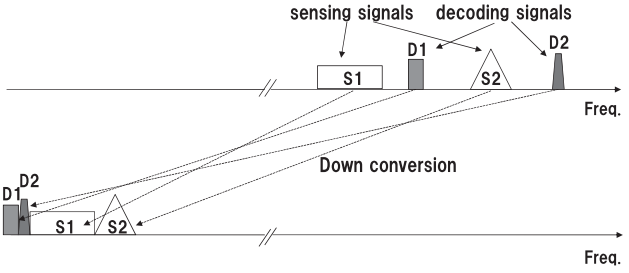

Fig. 3 Example of the frequency alignment of multiple signals (D1,D2: decoding signals, S1,S2: sensing signals).

3.1 System Model

The protocol-free signal processing decides the priorities and frequency alignment of multiple signals. The decoding signals are set at lower center frequencies than those of the sensing signals in the frequency alignment. The necessary control information such as the compression ratio, the initial seed of the random sequence generator, and parameters for tunable local oscillators and mixers is informed of each distributed flexible access point through wired access network.

At each distributed flexible access point, multiple signals are simultaneously received, filtered, and down converted to the IF band. Down conversion of each signal is done by tunable local oscillators and mixers of which parameters are set based on the received above control information. All down-converted signals are combined in the IF band, sampled by the proposed method, and transferred to the protocol-free signal processing unit.

The protocol-free signal processing unit conducts signal processing for the decoding and sensing using transferred data. Figures 2 and 3 show a simplified block diagram of a distributed flexible access point[†], and an example of the frequency alignment of multiple signals, respectively.

3.2 Proposed Sampling Method

Suppose that L decoding signals and Msensing signals are

[†]To reduce the number of RF components we have also proposed a new wideband receiver for a distributed flexible access point which uses only single local oscillators for down-converting multiple signals into IF band [29].

aligned in the IF band, and the total bandwidths of decoding signals and sensing signals are represented by B_{dec} and B_{sens}, respectively. For the convenience of the explanation, B_{grid} and B_{Nyq} are defined as $(4B_{dec} + 2B_{sens})$ and $(2B_{dec} + B_{sens})$, respectively. The purpose of the above setting is realizing Nyquist rate sampling against the decoding signals without aliasing from the sensing signals, and the compressed rate sampling against the sensing signals in a single ADC simultaneously.

The detailed procedure of proposed method proceeds as follows. First, B_{grid} rate sampling is conducted. Second, only some of even (or odd) samples are randomly discarded while all of odd (or even) samples are preserved. The rate of the random discard is controlled by the control parameter transferred from the protocol-free signal processing unit. The location of randomly discarded samples, which is determined by the random sequences generator, can be known to the protocol-free signal processing unit by sharing the initial seed of the random sequence generator. Figure 6(a) shows an example of the proposed sampling method in which all odd samples are preserved while some of even samples are randomly discarded. Hereafter, all of odd samples and remained even samples are called fixed samples and random samples, respectively. Those fixed and random samples are transferred to the protocol-free signal processing unit through wired access line.

The mathematical description of the proposed method is as follows. For simplicity, we consider multiple sparse signals in the frequency domain. The IF band signal $\mathbf{X}$ (= $\mathbf{\Psi s}$) is sparsely represented in the frequency domain. The basis matrix $\mathbf{\Psi}$ is $N \times N$ inverse Fourier transform, and $\mathbf{s}$ is the $N \times 1$ coefficient vector of $\mathbf{X}$ in the frequency domain. Note that $\mathbf{s}$ has sequential nonzero values in the lower frequency region and randomly sparse nonzero values in the higher frequency region (ex. $\mathbf{s} = [1111100100010001]$). The $K \times N$ projection matrix $\mathbf{\Phi}$ has the following sparse representation.

$$\mathbf{\Phi} = \begin{bmatrix} 1 & 0 & 0 & 0 & 0 & \cdots & 0 \\ 0 & 0 & 1 & 0 & 0 & \cdots & 0 \\ 0 & 0 & 0 & 1 & 0 & \cdots & 0 \\ 0 & 0 & 0 & 0 & 1 & \cdots & 0 \\ \vdots & \vdots & \vdots & \vdots & \vdots & \ddots & \vdots \\ 0 & 0 & 0 & 0 & 0 & 0 & 1 \end{bmatrix}. \tag{3}$$

Note that each column indicates a sample point of the signal. Every odd sample is preserved while some of the even samples are randomly discarded.

Then, compressed sensing matrix $\mathbf{\Theta}$ (= $\mathbf{\Phi\Psi}$) becomes $K \times N$ matrix which consists of every odd row and randomly selected even rows of the inverse Fourier transform matrix. Projection vector $\mathbf{Y}$ is represented as $\mathbf{\Theta s}$ and signal reconstruction becomes the inverse problem of $\mathbf{s} = \mathbf{\Theta}^{-1}\mathbf{Y}$. This inverse problem is solvable as an l1-norm minimization problem because $\mathbf{s}$ is sparse and $\mathbf{\Theta}$ consists of randomly selected rows of the inverse Fourier transform matrix[†].

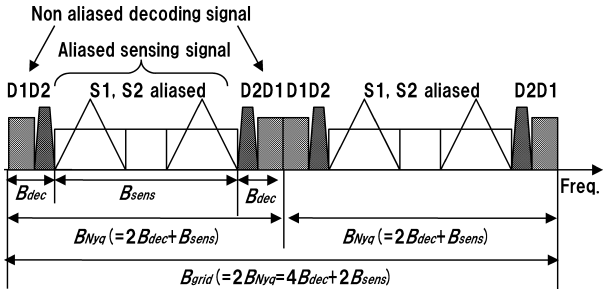

Fig. 4 Frequency domain representation of fixed samples.

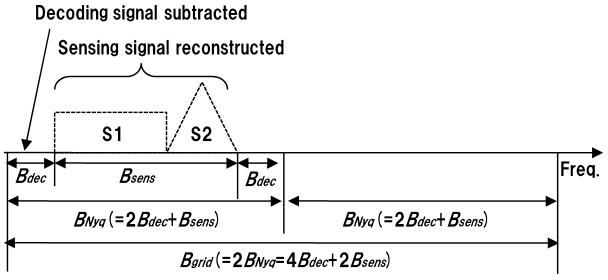

Fig. 5 Frequency domain representation of reconstructed sensing signals from decoding signal subtracted fixed and random samples.

3.3 Decoding and Sensing

Using transferred fixed and random samples from distributed flexible access points, the protocol-free signal processing unit conducts decoding and sensing process as below.

First, the decoding signals are decoded using only fixed samples, which is equivalent to B_{Nyq} rate sampling. Note that aliasing of the sensing signals occurred due to the insufficient sampling rate. However, it does not cause interference to the decoding signals. Therefore, the decoding signals can be decoded by using conventional decoding algorithms without aliasing. Figures 4 and 6(b) shows an example of fixed samples in the frequency and the time domain, respectively. Although the aliasing of the sensing signals occurred due to the insufficient sampling rate, the decoding signal parts are intact. Subsequently, the Nyquist-rate decoding performance is achieved for the decoding signals. Second, part of the decoding signals is subtracted from both fixed and random samples. Figure 6(c) shows an example that the decoding signals are subtracted from fixed and random samples shown in Fig. 6(a). Third, the sensing signals are reconstructed using both fixed and random samples of which decoding signals are subtracted. The reconstruction is done by solving the l1-norm minimization problem. Figure 5 shows an example of the reconstructed signal in the

[†]Compressed sensing theory proved that randomly permutated Fourier ensembles satisfy RIP. Therefore, we can use the randomly selected rows inverse Fourier transform matrix as a sensing matrix because Fourier ensembles and inverse Fourier ensembles have the identical statistical characteristics.

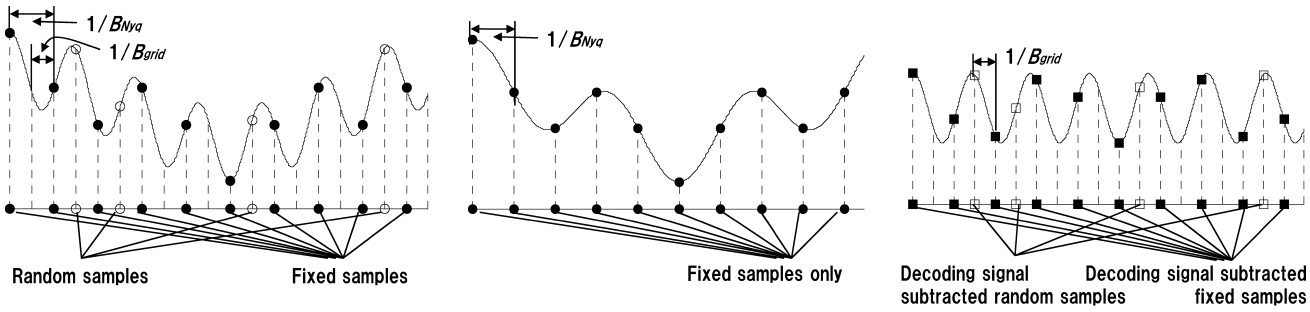

(a) (b) (c)

Fig. 6 Example of the proposed sampling method: (a) Fixed and random samples, (b) Fixed samples only, (c) Decoding signal subtracted fixed and random samples.

frequency domain. Note that only sensing signals are reconstructed because the decoding signals are removed. Fourth, the sensing signals are identified in the reconstructed signal by the conventional spectrum sensing algorithm such as energy detection.

4. Simulation and Experiment Results

This section uses computer simulations and experiments to answer the following questions: 1) Is Nyquist-rate decoding performance guaranteed for the decoding signals? 2) How much compression ratio can be achieved for the sensing signals in terms of E_b/N_o? 3) What level of signal occupancy is allowed for stable signal reconstruction? 4) Does the proposed method work in the real world experiments? 5) How much performance enhancement is achieved by increasing the number of processed symbols when the signal energy is low?

4.1 Simulation Results

Simulations were performed on unmodulated pure real tone signals with flat band-limited Gaussian noise. Simulation parameters are given in Table 1. The total bandwidths of decoding signals (B_{dec}) and sensing signals (B_{sens}) were set to 1 MHz and 9 MHz, respectively. The number of decoding signals was set to 10 and the number of sensing signals was varied from 5 to 25. The bandwidth of one tone signal was set to 0.1 MHz. This means that the decoding signal band was fully occupied while the sensing signal band was partially occupied. The decoding signals were directly decoded from the sampled data, and the sensing signals were identified by frequency domain energy detection after the reconstruction process. The threshold for energy detection over non-fading AWGN channel was derived from the below Eq. (4) [30] in order that the false alarm rate (P_f) yields 0.01.

$$P_f = \Gamma(N/2, \lambda/2\sigma^2)/\Gamma(N/2) \tag{4}$$

where, λ, $\Gamma(\cdot)$, and $\Gamma(\cdot,\cdot)$ are the threshold, gamma function, and incomplete gamma function, respectively. N and σ^2 are set to 2 and 1, respectively.

Table 1 Simulation parameters.

Modulation:	Real Tone	Whole bandwidth	10 MHz
Channel	Non-fading AWGN	One tone signal bandwidth	0.1 MHz
Eb/No	10 – 20 dB	Whole decoding signal bandwidth	1 MHz
Signal occupancy rate	0.2 - 0.5	Whole sensing signal bandwidth	9 MHz
Compression ratio	0.55 - 1		

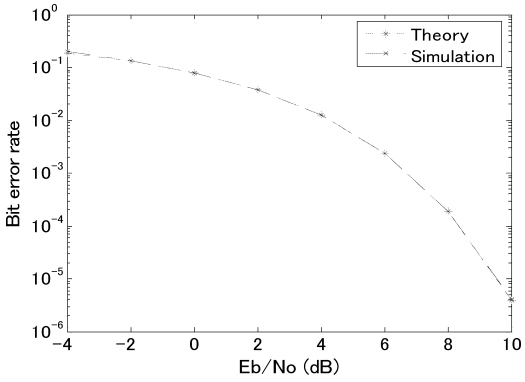

Fig. 7 Bit error rate comparison of the decoding signals between the theory and proposed method.

Figure 7 shows the bit error rate comparison of the decoding signals. The performance curve well matches the theoretical performance because the decoding signals were subjected to be sampled at the Nyquist rate. The plot shows that the proposed sampling method guarantees Nyquist-rate decoding performance for the decoding signals. Therefore, we can answer the above stated first question in the positive.

Figure 8 shows the detection success rate (P_d) with 10 sensing signals. All curves show poor performance at low compression ratio. This is due to the fact that reconstruction fails if the number of samples is insufficient. However, P_d converges to 1 as the compression ratio increases except for the E_b/N_o curve of 10 dB. This is because the

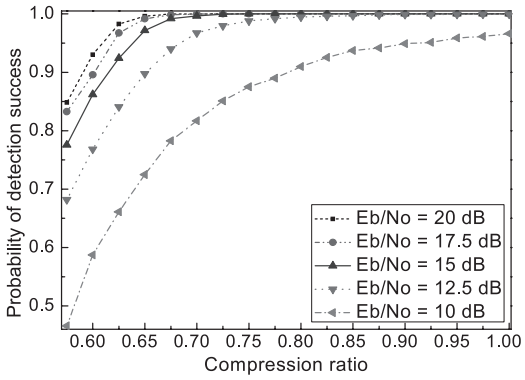

Fig. 8 Probability of detection success in terms of E_b/N_o.

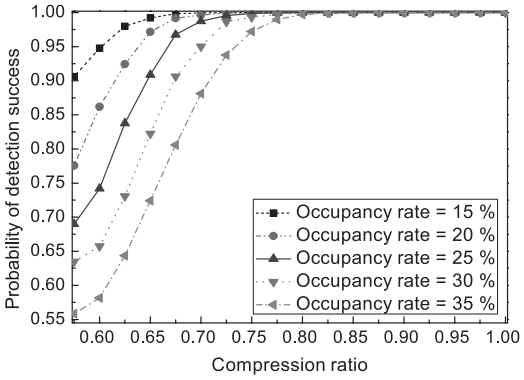

Fig. 10 Probability of detection success in terms of occupancy rate.

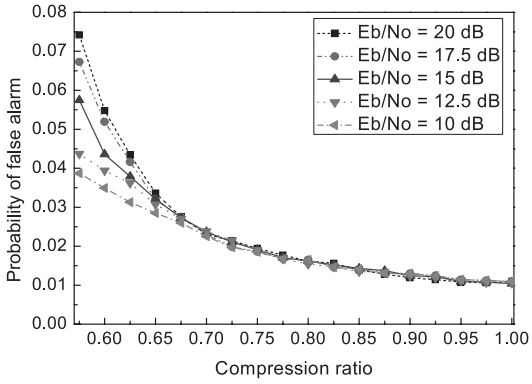

Fig. 9 Probability of false alarm in termes of E_b/N_o.

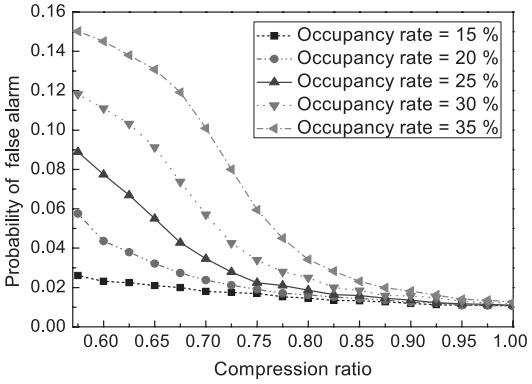

Fig. 11 Probability of false alarm in termes of occupancy rate.

signal no longer exhibits sparsity at this E_b/N_o value due to the increased noise power. Figure 9 shows the detection false alarm rate (P_f) with 10 sensing signals. The interesting observation is that P_f increases as E_b/N_o increases when the compression ratio is low. This arises from the fact that the reconstruction error, created by the paucity of sample numbers, yields stronger energy at the wrong point as E_b/N_o increases. However, for all curves, P_f decreases and converges to a point slightly higher than 0.01 as the compression ratio increases. P_f slightly exceeds the theoretical result due the added noise imposed by reconstruction. Considering the results of Fig. 8 and Fig. 9, it is concluded that the proposed method can enable the approximately 70 percent of compression ratio when E_b/N_o is higher than 15 dB with only a slight increase in the false alarm rate. This answers the above stated second question.

The next two simulations used the same parameters as the preceding simulations; E_b/N_o was set to 15 dB and the number of sensing signals was varied from 5 to 25, which yields the signal occupancy rate of 0.15 to 0.35 given 10 decoding signals among a total of 100 signal bands. Figure 10 shows the detection success rate of the sensing signals. As the occupancy rate increases, the number of samples needed for signal reconstruction increases. Therefore, P_d shows worse performance as the occupancy rate increases at the same compression ratio. Figure 11 shows the detection false alarm rate of the sensing signals. P_f increases with the occupancy rate, and decreases as the compression ratio increases as expected. The third question is answered as follows from the results shown in Fig. 10 and Fig. 11. Occupancy rates of up to 30% offer reasonable performance (less than 70 percent of compression ratio with tolerable detection error rates and false alarm rates).

Table 2 Experiment parameters.

Modulation	FSK	Whole bandwidth	8.27 MHz
Channel	Non-fading AWGN	One RFID tag signal bandwidth	0.3 MHz
Es/No	-10 – 20 dB	Whole decoding signal bandwidth	1.73 MHz
Signal occupancy rate	0.0726	Whole sensing signal bandwidth	6.54 MHz
Compression rate	0.625 - 1	Number of averaged symbols	2 - 20

4.2 Experiment Results

Experiments were performed on 310 MHz band FSK signals transmitted by radio frequency identification (RFID) tags [1]. Experiments parameters are given in Table 2. Received signals are down-converted into IF band signal. The bandwidth of a RFID tag, total bandwidths of decod-

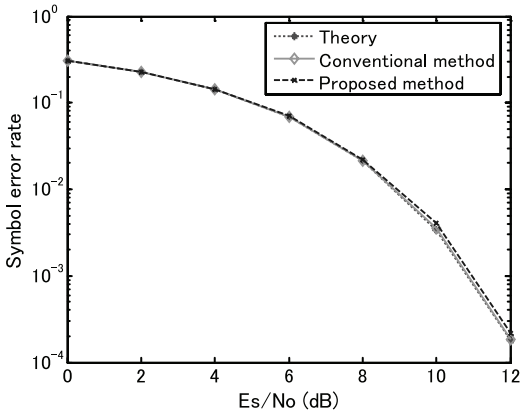

Fig. 12 Symbol error rate comparison of the decoding signal among the theory, conventional method, and proposed method.

ing signals and sensing signals were 0.3 MHz, 1.73 MHz, and 6.54 MHz, respectively. The channel between RFID tags and the distributed flexible access point was non-fading AWGN channel. For the convenience of the experiments, low channels and high channels of RFID tags were regarded as the decoding signals and the sensing signals, respectively. This means that signals at low channels are decoded with Nyquist rate sampling while signals at high channels are identified with compressed rate sampling. The decoding signals were directly decoded, and the sensing signals were identified by frequency domain energy detection after the reconstruction process. Considering the above provided simulation results, the threshold for energy detection is set to slightly higher than Eq. (4) to suppress the increased noise caused by the reconstruction process. Specifically, the threshold was set for P_f to be 0.01 when the compression ratio is 0.7.

Figure 12 shows the symbol error rate comparison of the decoding signal between the theory and experiments. Experiments are performed by the conventional Nyquist sampling method and the proposed sampling method. In the experiment of the conventional method, only downconverted decoding signal is sampled at the Nyquist rate without combining with the sensing signals. In the experiment of the proposed method, the decoding signal and the sensing signals are combined in IF band, and sampled by the proposed method. The performance curve of the proposed method well matches the theoretical and the conventional method because the decoding signal of the proposed method were subjected to sampled at the Nyquist rate without aliasing from the sensing signals as explained in Sect. 3. Likewise the simulation result in Fig. 7, this plot shows that the proposed sampling method guarantees Nyquist-rate decoding performance for the decoding signal.

The detection success rate and the false alarm rate of the sensing signals are given in Fig. 13 and Fig. 14, respectively. Both were obtained when a single decoding signal and a single sensing signal were transmitted. Curves in both figures show similar features with those of simulation results. Approximately, 70 percent of compression ratio can

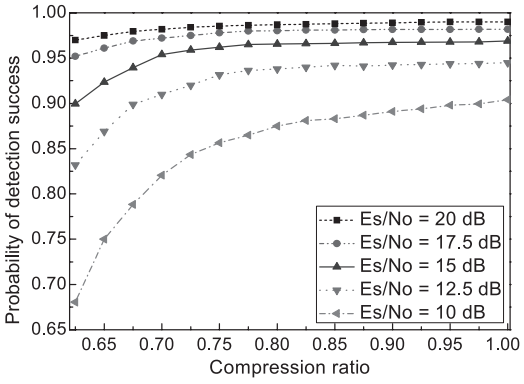

Fig. 13 Probability of detection success in terms of E_s/N_o.

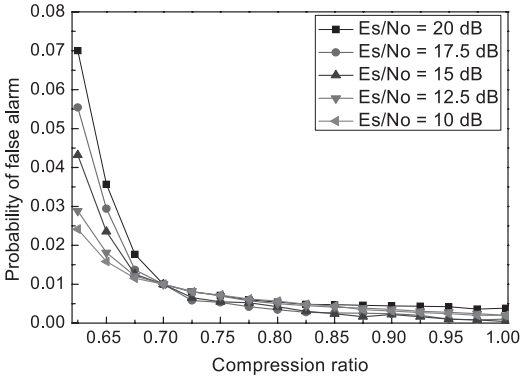

Fig. 14 Probability of false alarm in termes of E_s/N_o.

be reduced when E_S/N_o is higher than 17.5 dB. From the results shown in Fig. 13 and Fig. 14, we can answer the above stated fourth question in the positive.

To investigate the performance enhancement by noise averaging method at low E_S/N_o, L consecutive reconstructed sensing signals are averaged. Figures 15 and 16 show P_d and P_f of sensing signals at 10 dB E_S/N_o, respectively. The number of averaged consecutive signals was set to be 2, 4, and 6. In each curve, the threshold was set for P_f to be 0.01 when the compression ratio is 0.7. It is clearly confirmed that P_d is enhanced as the number of averaged signals is increased. It is also confirmed that P_f is maintained to be below 0.01 when the compression ratio is over 0.7.

For further analysis of the performance enhancement by the noise averaging, an additional experiment was conducted by increasing the number of averaged signals up to 20 with various E_S/N_o levels. Threshold fixed for P_f to be 0.01 when the compression ratio is 0.7. Figure 17 shows P_d of this experiment. It is confirmed that the performance enhancement is achieved by noise averaging at low E_S/N_o region. In particular, 0.99 of P_d is obtained at 2.5 dB E_S/N_o by averaging 20 consecutive reconstructed signals.

Results given from Figs. 15 to 17 answer the above stated fifth question by showing the possibility of the performance enhancement by noise averaging with the sacrifice of processing time.

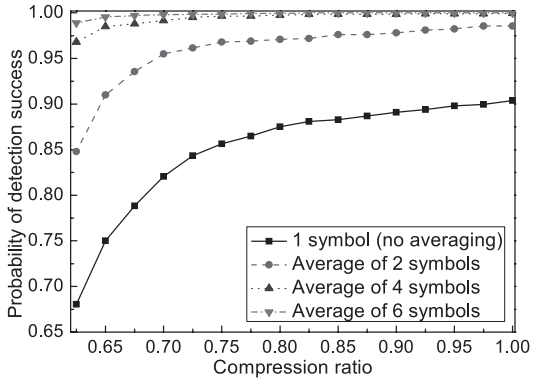

Fig. 15 Probability of detection success with noise averaging (E_s/N_o = 10 dB).

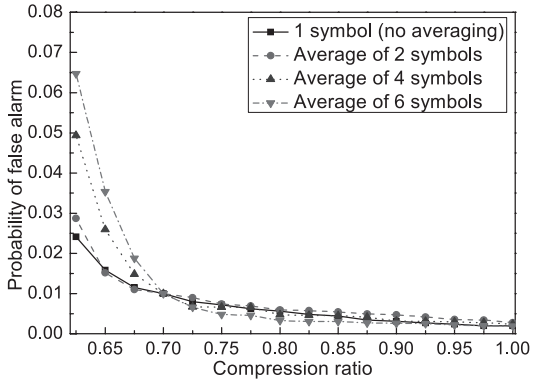

Fig. 16 Probability of false alarm with noise averaging (E_s/N_o = 10 dB).

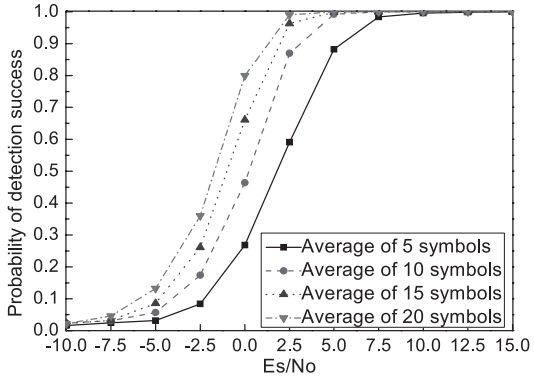

Fig. 17 Probability of detection success in terms number of E_s/N_o (P_f = 0.01 and compression ratio = 0.7).

5. Conclusion

To realize a highly flexible and efficient radio wave data compression of a heterogeneous network system, a combined Nyquist and compressed sampling method is proposed using the compressed sensing theory. Decoding the known signals yields the theoretical performance. Regarding the detection of unknown signals, it is shown that they can be detected with the reduced sampling numbers made possible by the compressed sensing reconstruction method. In particular, 70 percent of compression ratio is achieved with the appropriate E_b/N_o with only slight increase in false alarm rate. It is also revealed that the performance of the proposed method gradually decreases as the occupancy rate increases due to the nature of compressed sensing. However, the proposed method offers a significant decrease in the sampling rate if the signal occupancy rate is less than 0.3. Experiments are also conducted with 310 MHz band RFID tags with slightly enhanced threshold to suppress the increased noise caused by reconstruction process. Experiment results also revealed that the proposed method guarantees the Nyquist-rate decoding performance for the decoding signal and enables approximately 70 percent of compression ratio. Moreover, we confirm the further possibility of the performance enhancement by noise averaging with the sacrifice of the processing time. In particular, it is confirmed that 0.99 of P_d is obtained at 2.5 dB E_S/N_o by averaging 20 consecutive reconstructed signals.

References

[1] H. Ichikawa, M. Shimizu, and K. Akabane, "Appliance defined ubiquitous network," Proc. International Symposium on Applications and the Internet Workshop, pp.20–23, Jan. 2007.
[2] H. Ichikawa, M. Shimizu, and K. Akabane, "Ubiquitous networks with radio space extension over broadband networks," IEICE Trans. Commun., vol.E90-B, no.12, pp.3445–3451, Dec. 2007.
[3] H. Shiba, K. Akabane, T. Yamada, and K. Uehara, "A unified wireless platform architecture for a wide variety of wireless systems," Proc. SDR'09 Technical Conference, Dec. 2009.
[4] N. Takahashi, K. Akabane, M. Matsuo, M. Ohta, M. Harada, and K. Okada, "Technologies towards networked objects and events in the real world," NTT Technical Review, no.5, May 2009.
[5] K. Xu, X. Sun, J. Yin, H. Huang, J. Wu, X. Hong, and J. Lin, "Enabling ROF technologies and integration architectures for in-building optical-wireless access networks," IEEE Photonics Journal, vol.2, no.2, pp.102–112, April 2010.
[6] A. Chowdhury, H. Chien, Y. Hsueh, and G. Chang, "Advanced system technology and field demonstration for in-building optical-wireless network with integrated broadband services," J. Lightwave Technol., vol.27, no.12, pp.1920–1927, June 2009.
[7] A. Bekkali, P. Dat, K. Kazura, K. Wakamori, M. Mastumoto, T. Higashino, K. Tsukamoto, and S. Komaki, "Performance evaluation of an advanced DWDM RoFSO system for transmitting multiple RF signals," IEICE Trans. Fundamentals, vol.E92-A, no.11, pp.2697–2705, Nov. 2009.
[8] D. Donoho, "Compressed sensing," IEEE Trans. Inf. Theory, vol.52, no.4, pp.1289–1306, April 2006.
[9] R. Baraniuk, "Compressive sensing [Lecture notes]," IEEE Signal Process. Mag., vol.24, no.4, pp.118–121, July 2007.
[10] E. Candes and M. Wakin, "An introduction to compressive sampling," IEEE Signal Process. Mag., vol.25, no.2, pp.21–30, March 2008.
[11] J. Bobin, J. Starch, and R. Ottensamer, "Compressed sensing in astronomy," IEEE J. Sel. Top. Sign. Process., vol.2, no.5, pp.718–726, Oct. 2008.
[12] M. Lustig, D. Donoho, J. Santos, and J. Pauly, "Compressed sensing MRI," IEEE Signal Process. Mag., vol.25, no.2, pp.72–82, March 2008.
[13] M. Duarte, M. Davenport, D. Takhar, J. Laska, T. Sun, K. Kelly, and R. Baraniuk, "Single-pixel imaging via compressive sampling," IEEE Signal Process. Mag., vol.25, no.2, pp.83–91, March 2008.

[14] J. Paredes, G. Arce, and Z. Wang, "Ultra-wideband compressed sensing: Channel estimation," IEEE J. Sel. Top. Sign. Process., vol.1, no.3, pp.383–395, Oct. 2007.
[15] Z. Tian and G. Giannakis, "Compressed sensing for wideband cognitive radios," Proc. International Conference on Acoustics, Speech, and Signal Processing (ICASSP), pp.IV/1357–1360, April 2007.
[16] J. Haupt and R. Nowak, "Compressive sampling for signal detection," Proc. International Conference on Acoustics, Speech, and Signal Processing (ICASSP), pp.III/1509–1512, April 2007.
[17] L. Gueguen, B. Sayrac, and D. Depierre, "Spectrogram reconstruction from random sampling: Application to the GSM band sensing," Proc. IEEE International Conference on Communications (ICC), June 2009.
[18] Y. Wang, A. Pandharipande, Y. Polo, and G. Leus, "Distributed compressive wide-band spectrum sensing," Proc. IEEE Information Theory Application (ITA), pp.1–4, Feb. 2009.
[19] Z. Yu, S. Hoyos, and B. Sadler, "Mixed-signal parallel compressed sensing and reception for cognitive radio," Proc. International Conference on Acoustics, Speech, and Signal Processing (ICASSP), pp.3861–3864, March 2008.
[20] Z. Yu, X. Chen, S. Hoyos, B. Sadler, J. Gong, and C. Qian, "Mixed-signal parallel compressive spectrum sensing for cognitive radios," International Journal of Digital Multimedia Broadcasting, vol.2010, pp.1–10, Jan. 2010.
[21] E. Candes and T. Tao, "Decoding by linear programming," IEEE Trans. Inf. Theory, vol.51, no.12, pp.4203–4215, Dec. 2005.
[22] E. Candes, J. Romberg, and T. Tao, "Robust uncertainty principles: Exact signal reconstruction from highly incomplete frequency information," IEEE Trans. Inf. Theory, vol.52, no.2, pp.489–509, Feb. 2006.
[23] E. Candes and T. Tao, "Near optimal signal recovery from random projections: Universal encoding strategies?" IEEE Trans. Inf. Theory, vol.52, no.12, pp.5406–5425, Dec. 2006.
[24] E. Candes and J. Romberg, "l1-magic: Recovery of sparse signals via convex programming," Online: www.l1-magic.org. Oct. 2005.
[25] J. Tropp and A. Gilbert, "Signal recovery from random measurement via orthogonal matching pursuit," IEEE Trans. Inf. Theory, vol.53, no.12, pp.4655–4666, Dec. 2007.
[26] E. Candes, "The restricted isometry property and its implications for compressed sensing," Compte Rendus de l'Academie des Sciences, Series I, vol.346, no.9-10, pp.589–592, May 2008.
[27] R. Baraniuk, M. Davenport, R. Devore, and M. Wakin, "A simple proof of the restricted isometry property for random matrices," Constructive Approximation, vol.28, no.3, pp.253–263, 2008.
[28] E. Candes, J. Romberg, and T. Tao, "Robust uncertainty principles: Exact signal reconstruction from highly incomplete frequency information," IEEE Trans. Inf. Theory, vol.52, no.2, pp.489–509, Feb. 2006.
[29] T. Kaho, Y. Yamaguchi, H. Shiba, D. Lee, T. Yamada, M. Kawashima, and K. Uehara, "Proposal of a wide-band and high dynamic range receiver for flexible wireless systems," IEICE Technical Report, MW2010-61, July 2010.
[30] F. Dighham, M. Alouini, and M. Simon, "On the energy detection of unknown signals over fading channels," IEEE Trans. Commun., vol.55, no.1, pp.21–24, Jan. 2007.

Doohwan Lee received the B.S. degree and completed the M.S. course in electrical engineering from Seoul National University, Seoul, Korea in 2004 and 2006, respectively. He received the Ph.D. degree in electrical engineering and information systems from the University of Tokyo in 2009. He is currently working at NTT Network Innovation Laboratories as a postdoctoral researcher. His research interests include compressed sensing, flexible wireless system, software defined radio, and cognitive radio. He received the Japanese government Scholarship (Monbusho) during his Ph.D. studies.

Takayuki Yamada received the B.E. degree in Department of Electronics, Faculty of Engineering from Doshisha University, Kyoto, Japan, in 2005 and the M.E. degree in Communications and Computer Engineering, Graduate School of Informatics from Kyoto University, Kyoto, Japan, in 2007. Since joining NTT Network Innovation Laboratories in 2007, he has been engaged in research of flexible wireless system. He is a member of IEEE.

Hiroyuki Shiba received his B.E. and M.E. degrees from Gunma University, in 1995 and 1997, respectively. Since joining NTT Wireless Systems Laboratories, in 1997, he has been engaged in the research of data communication and software defined radio (SDR) systems. He is currently with NTT Network Innovation Laboratories. He is currently a Senior Research Engineer at NTT Network Innovation Laboratories. He received the young engineer Award from IEICE in 2001.

Yo Yamaguchi received the B.S. and M.S. degrees in chemistry, from Osaka University, Osaka, Japan, in 1989, and 1991, respectively. In 1991, he joined NTT Radio Communication Systems Laboratories, Yokosuka, Japan, where he was engaged in research and development on MMIC's. From 1999 to 2001, he was an Associate Manager at STE Telecommunication Engineering Co., Ltd., where he served as a Technical Consultant on wireless communications. Since 2001, he has been a Senior Research Engineer at NTT Network Innovation Laboratories, Yokosuka, Japan. He is currently involved in the design of MMICs. Mr. Yamaguchi is a member of the IEEE.

Kazuhiro Uehara received the B.E., M.E., and Ph.D. degrees from Tohoku University, in 1987, 1989, and 1992, respectively. In 1992, he joined Nippon Telegraph and Telephone Corporation (NTT) and was engaged in the research of array antennas, active antennas and indoor propagation in millimeter-wave and microwave frequency bands. From 1997 to 1998, he was a Visiting Associate at the Department of Electrical Engineering, California Institute of Technology, CA. From 2003, he has been a Part-time Lecturer at the Department of Electrical Engineering, Tohoku University. He is currently a Senior Research Engineer, Supervisor, Group Leader at NTT Network Innovation Laboratories, where he engages in the research and development of software defined radio and cognitive radio systems, and millimeter-wave multi-Gigabit wireless systems. He is currently serving as Chair of Technical Committee on Software Radio, IEICE Communication Society. He received the Young Engineer Award and the Excellent Paper Award from IEICE, the 1st YRP Award, and the 18th Telecom System Technology Award from the Telecommunications Advancement Foundation in 1995, 1997, 2002, and 2003 respectively. He is a senior member of IEEE.